Transformer-Based Current-Gain-Boost Technique for Dual-Band and Wide-Band Receiver Front-Ends

Alan W.L. Ng and Howard C. Luong

Hong Kong University of Science and Technology, Clear Water Bay, Hong Kong

***Abstract* — Dual-band and wide-band receiver-front-ends (RFEs) using transformer-based current-gain-boost techniques are designed in 0.13µm CMOS. With a single switchable 3-coil transformer, the first dual-band RFE prototype measures NF of 2.5dB and 3.5dB and voltage gain of 20.7dB and 17dB at 1.7GHz and 3.8GHz, respectively. The second wide-band RFE achieves 0dBm IIP3 with 4dB NF and 13dB voltage gain over a frequency range from 2GHz to 5GHz.**

***Index Terms* — Receiver, transformer, receiver front-end, RFE, LNA, dual band, wideband, passive mixer**

I. Introduction

Direct-conversion receivers employing passive current-driven mixers have recently attracted widespread attention due to its superior 1/f noise and linearity performance [1-3]. In this architecture, a passive current-driven mixer commutates the RF current output from a low-noise transconductance amplifier (LNTA) and delivers the down-converted current to a low-input-impedance current buffer or trans-impedance amplifier. Current-to-voltage and voltage-to-current conversions in conventional receiver front-ends (RFEs) are usually removed to improve its linearity. However, the input transconductance (g_m) would need to be increased accordingly to provide sufficient gain and to reduce noise. Having additional current gain between the LNTA and the current-driven passive mixer is therefore highly desirable.

II. Transformer-Based Current-Gain-Boosted Techniques

Fig. 1 shows the proposed current-gain-boost RFE architecture with two key features. First, the RFE employs a transformer as the load of the LNTA and as interface to the passive mixer to achieve additional current gain. Second, the RFE can be reconfigured either for narrow-band applications with high gain and low NF or for wide-band applications with high linearity by simply controlling the series capacitor C_S.

For narrow-band applications in which the NF becomes critical, the RFE can be configured as shown Fig. 1(b) in which C_S is connected in series with Z_m. In this configuration, the total current gain consists of two parts. The first part is a current gain of Q, which is achieved as

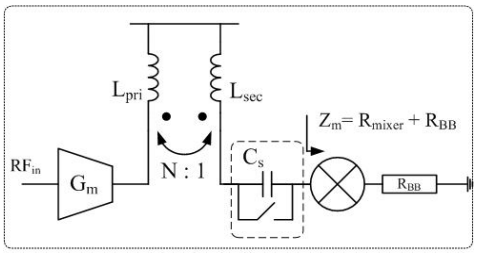

(a) Block diagram

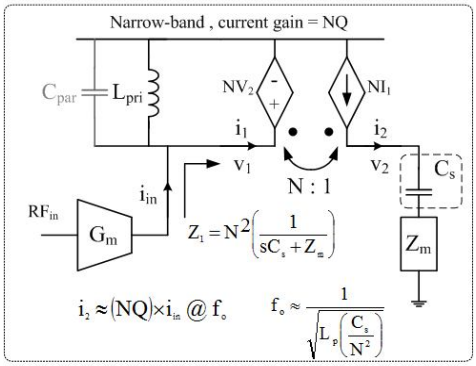

(b) Equivalent Model With C_s

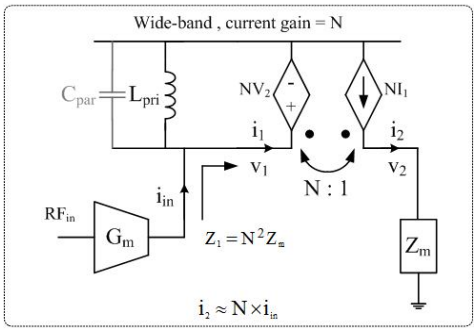

(c) Equivalent Model Without C_s

Fig. 1. Proposed Current-gain-boost technique (a) Block Diagram (b) Equivalent Model With C_s (c) Equivalent model without C_s

long as the transformed impedance of C_S is designed to resonate with L_{pri}, where Q is the equivalent quality factor of the parallel tank [2]. The second part is an additional current gain of N, where N is the ratio of L_{pri} and L_{sec}, due to the current transfer from the primary coil to the secondary coil. As a result, a total current gain of NQ is achieved at the input of the mixer, and effectively the

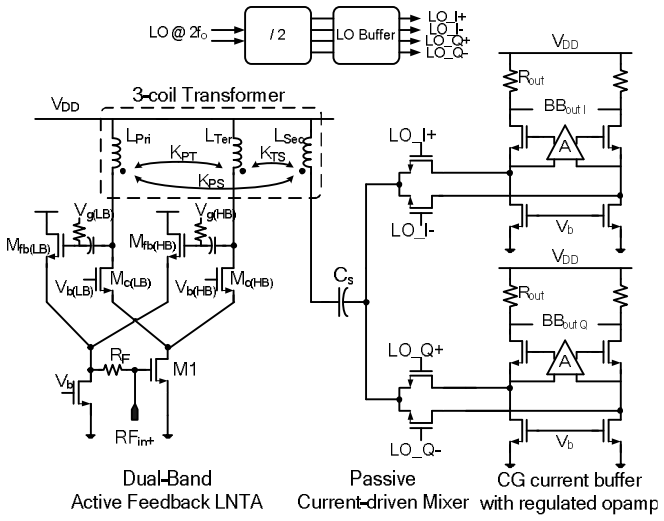

Fig. 2 Current-gain-boost low-noise dual-narrow-band RFE with a 3-coil differential transformer (In actual implementation, LNTA is differential and the mixer are double-balanced)

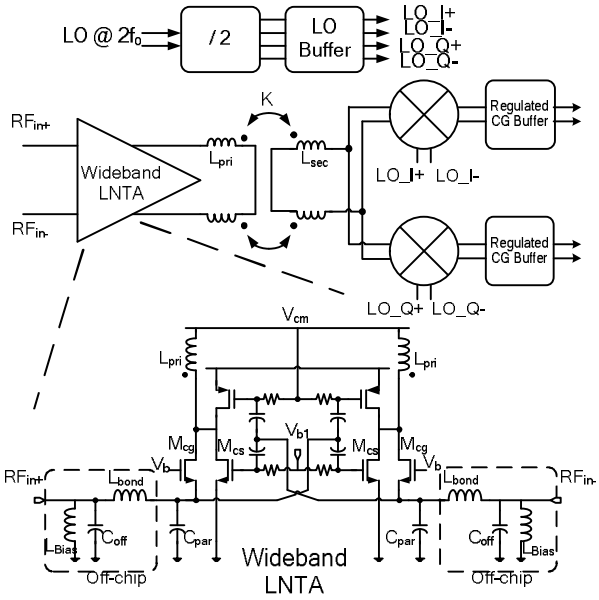

Fig. 3 Current-gain-boost high-linearity wide-band RFE

input transconductance g_m and thus the gain are boosted by the same factor (NQ). It is critical to minimize both Z_m and parasitic capacitance to maximize Q and to ensure that the capacitive current is dominated by the transformed impedance of C_S.

On the other hand, for wideband applications in which the linearity is typically more critical than the noise figure, the RFE can be configured as shown Fig. 1(c) in which C_S is shorted. Provided that the impedance of L_{pri} is sufficiently high, a relatively wide-band current gain of N is achieved by terminating the transformer with low impedance Z_m of the mixer and the baseband circuitry. Maintaining low impedance at the output of LNTA reduces signal swing and improves linearity.

III. Circuit Design and Implementation

As a proof of concepts, two RFE versions are designed and fabricated in a 0.13µm CMOS process, one of which is for low-noise narrow-band applications with current gain of NQ while the other is for high-linearity wide-band applications with current gain of N.

Fig. 2 shows the detailed schematic of the narrow-band RFE. To achieve dual-band operation, a single 3-coil differential transformer is employed. The primary and tertiary coils L_{pri} and L_{ter} are connected to the outputs of the LNTA via two switchable cascode devices $M_{c(LB)}$ and $M_{c(HB)}$ while the secondary coil L_{sec} with the smallest number of turns is connected in series with the passive mixer via C_S. The impedance of C_S is transformed to the primary and the tertiary coil and forms parallel resonant tanks, which provides current gain at the two respective resonant frequencies. Conveniently, the transformer's secondary coil also functions effectively as combining or selection of the outputs of the primary and the tertiary coils to drive the same mixer path. When the transformer is resonant, its impedance is real. Active-feedback [4] is used at the LNTA so that 50-ohm input matching is obtained at the tank's resonant frequency. Band switching is achieved by tuning on the respective active-feedback paths ($M_{fb(LB)}$, $M_{fb(HB)}$) and cascode devices ($M_{c(LB)}$, $M_{c(HB)}$). 3-bits binary-weighted switched-capacitor arrays (SCA) are connected to the primary and the tertiary coils and are used for fine frequency tuning.

Fig. 3 shows the block diagram and schematic of the RFE for high linearity and wide band. To achieve high linearity, the signal swing and the impedance at the output of the LNTA is kept low by optimizing the low impedance of the mixer and the regulated common-gate (CG) current buffer. For the LNTA, the wide-band common-gate transistor (M_{cg}) provides input matching while the ac-coupled common-source transistors (M_{csn}, M_{csp}) further increase the input stage g_m. The center-tap of the primary coil senses the common-mode signal and is fed back to the PMOS transistors for common-mode feedback. An off-chip third-order filter (C_{par}, L_{Bond}, C_{off}) is used to increase the input matching bandwidth.

A common-gate (CG) current buffer with regulated opamp is used to reduce the input impedance of the baseband circuitry. At low frequency, the equivalent input impedance is equal to $1/(g_m A_{amp})$ where g_m is the input gm of the CG transistor and A_{amp} is the gain of the regulated opamp. Compared to the traditional trans-impedance stage formed by an opamp and resistor feedback, the regulated

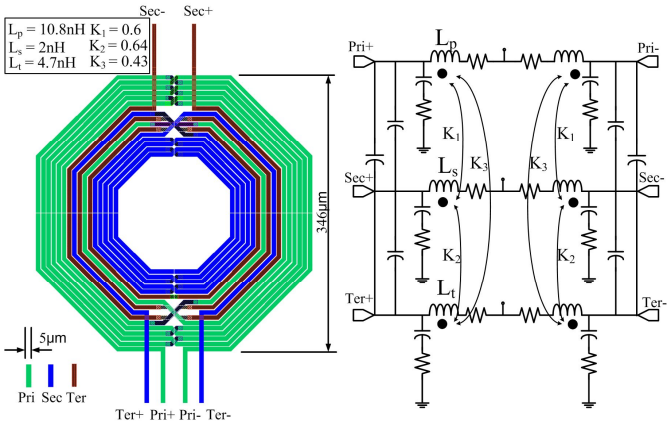

Fig. 4 Layout and model of the single 3-coil transformer for the dual-narrow-band RFE

CG buffer provides lower input impedance and decouples the trade-off between the input impedance and the trans-impedance gain. As the gain requirement of the opamp is reduced, a simple single-stage opamp can be used. Current-mode-logic (CML) divider and LO buffers generate IQ LO signals for the mixer.

The layout and the model of the differential 3-coil transformer used in the dual-narrow-band RFE are shown in Fig. 4. Only top metal layer is used for the spirals to maximize the quality factor Q and the self-resonant frequency. The transformer has an outer length of 346μm with 5μm metal width and 1.5μm spacing. The transformer is modeled with three individual pi models with magnetic and capacitive coupling between coils. Individual testing structure is tested with on-wafer probing using 4-port network analyzer (Agilent N5230A), and the network analyzer is calibrated up to the probe-tip with Cascade Microtech ISS Substrate. Important measured parameters are listed on the figure.

IV. Experimental Results

The dual-narrow-band and the wide-band RFEs are fabricated in a 0.13μm CMOS process, and the die micrographs are shown in Fig. 5, which occupy 1.2mm^2 and 1.8mm^2, respectively. Fig. 6 plots the measured S11, and Fig. 7 shows the measured voltage conversion gain and DSB NF with IF of 5MHz.

For the dual-narrow-band RFE, S_{11} is measured to be below -10dB from 1.34GHz to 1.88GHz for the low band and from 3.19GHz to 4.10GHz for the high band with fine tuning SCAs. Loaded with 200-ohm output impedance R_{out}, the gain and NF at 1.7GHz LO are 20.7dB and 2.5dB while those at 4GHz LO are 17dB and 3.4dB, respectively. Two-tone tests with 5MHz spacing measure IIP3 of -13.6dBm at 1.7GHz and -11dBm at 4GHz. With 1.2V

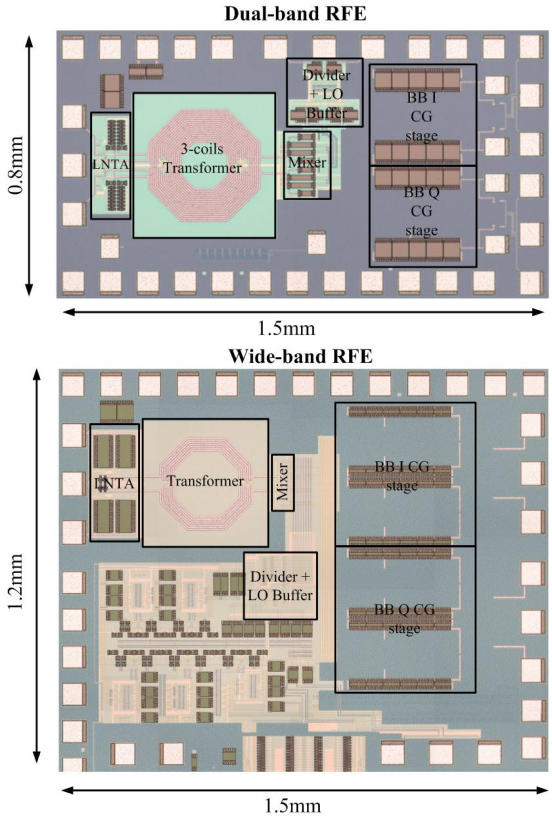

Fig. 5 Die micrographs

supply, the narrow-band RFE consumes a total current of 19mA, out of which 10mA is for the LNTA and 9mA is drawn by the IQ common-gate buffer and the regulated opamp. With the assumptions that the mixer's conversion gain coefficient is equal to $2/\pi$, R_{out} is 200 ohm, and the effective g_m of the input stage is 60mS, the additional current gain at the low band and the high band are measured to be 9dB and 5.5dB, respectively.

The measured S_{11} of the wide-band RFE is below -10dB from 2GHz to 5GHz. At low frequency, the impedance of L_{pri} decreases and thus the gain decreases. Loaded with

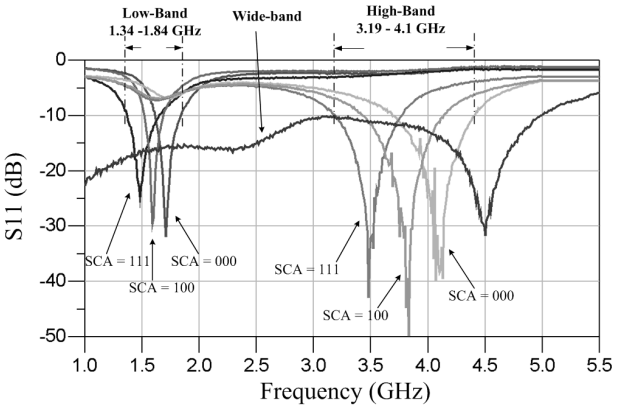

Fig. 6 Measured S_{11} of the dual-narrow-band and wide-band RFEs

TABLE I
PERFORMANCE SUMMARY AND COMPARISON

Parameter	Proposed Dual-band Receiver		Proposed Wide-band Receiver	Bagheri JSSCC'06 [3]	Zhan JSSCC'08 [5]	Blaakmeer JSSCC' 08 [6]	Feng JSSCC' 09 [7]
	Low-band	High-band					
RX Frequency [GHz]	1.34 - 1.84	3.19 – 4.1	2-5	0.8-6	2-5.8	0.5-7	2
Voltage Gain [dB]	20.7 (R_{out}=200Ω)	17 (R_{out}=200Ω)	13 (R_{out}=100Ω)	3-36	44	18	30
S_{11} [dB]	<-10	<-10	<-10	<-10	<-15	<-10	-22
IIP3 [dBm]	-13.6	-11	0	-3.5 1)	-21	-3	-12
DSB NF [dB]	2.5 - 3.4	3.2 - 4	3.6-4.5	5	3.4	4.5-5.5	3.1
Die Area [mm^2]	1.2		1.8	3.8	0.2 2)	<0.01 2)	1.1
Supply Voltage	1.2V			2.5V	2.7	1.2	1.5
Current [mA]	19	19	34				
LNA + MIXER				11.4	28	13.3 3)	8 3,4)
CMOS Technology	0.13µm			90nm	90nm	65nm	0.13µm

1) Mid-gain setting 2) Active area 3) LNA is single-ended input 4) Excluding baseband trans-impedance amplifier

100-ohm output impedance R_{out}, the voltage conversion gain and DSB NF are measured to be 13dB and 4dB with 3GHz LO, respectively. Two-tone tests with 5MHz spacing measure an IIP3 of 0dBm with 3GHz LO. With 1.2V supply, the wide-band RFE consumes a total current of 34mA, out of which 16mA is for the LNTA and 18mA is for the IQ common-gate buffer and the regulated opamp. More current is needed for the regulated buffer as compared to the narrow-band counterpart to improve the overall linearity. Assuming that the mixer's gain coefficient is equal to $2/\pi$, R_{out} is 100 ohm and the effective g_m of input stage is 100mS, the additional current gain is 2.9dB.

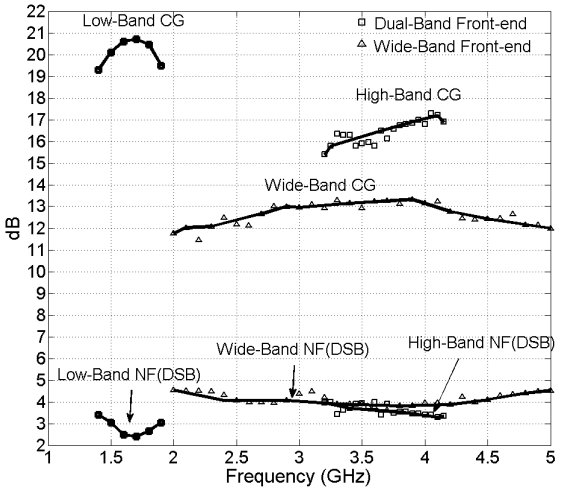

Fig. 7 Measured conversion gain and NF of the dual-narrow-band and wide-band RFEs

The performance of the proposed transformer-based dual-narrow-band and wide-band RFEs are summarized and compared with the published state-of–the-art CMOS RFEs as shown in Table I.

ACKNOWLEDGEMENT

This work was supported by the Hong Kong Innovation and Technology Funding ITS/187/10.

REFERENCES

[1] M. Valla, et al., "A 72-mW CMOS 802.11a direct conversion front-end with 3.5-dB NF and 200-kHz 1/f noise corner," *IEEE J. Sold State Circuits*, vol. 40, pp. 970-977, April 2005.

[2] A. Mirzaei, et al., "Analysis and Optimization of Current-Driven Passive Mixers in Narrowband Direct-Conversion Receivers," *IEEE J. Sold State Circuits*, vol. 44, pp. 2678-2688, Oct. 2009.

[3] R. Bagheri, et al., "An 800-MHz-6GHz software-defined wireless receiver in 90-nm CMOS," *IEEE J. Sold State Circuits*, vol. 41, pp. 2860-2876, Dec 2006.

[4] J. Borremans, et al., "Low-Area Active-Feedback Low-Noise Amplifier Design in Scaled Digital CMOS," *IEEE J. Sold State Circuits*, vol. 43, pp. 2422-2433, Nov. 2008.

[5] J-H. C. Zhan, et al., "A Broadband Low-Cost Direct-Conversion Receiver Front-End in 90 nm CMOS, "*IEEE J. Sold State Circuits*, vol. 43, pp. 1132-1137, May 2008.

[6] S.C. Blaakmeer, et al., " The BLIXER, a Wideband Balun-LNA-I/Q-Mixer Topology, "*IEEE J. Sold State Circuits*, vol. 43, pp. 2706-2715, Dec. 2008.

[7] Y. Feng, et al., " Design of a High Performance 2-GHz Direct-Conversion Front-End With a Single-Ended RF Input in 0.13µm CMOS "*IEEE J. Sold State Circuits*, vol. 44, pp. 1380-1390, May. 2009.